Journal of Arid Environments 72 (2008) 2093–2105

Contents lists available at ScienceDirect

Journal of Arid Environments

journal homepage: www.elsevier.com/locate/jaridenv

Assessing land-cover change and degradation in the Central Asian deserts using satellite image processing and geostatistical methods

A. Karnieli [a,*], U. Gilad [a], M. Ponzet [b], T. Svoray [c], R. Mirzadinov [d], O. Fedorina [e]

[a] The Remote Sensing Laboratory, Jacob Blaustein Institutes for Desert Research, Ben-Gurion University of the Negev, Sede Boker Campus 84990, Israel
[b] Department for Land Cultivation and Environmental Protection, Rostock University, Germany
[c] The Geographic Information Laboratory, Department of Geography and Environmental Development, Ben-Gurion University of the Negev, 84105, Israel
[d] Kazakh Academy of Transport and Communication, Shevcenko Street 97, Almaty 050012, Kazakhstan
[e] Kazakh State Scientific Production Center of Land Management Complex Prospecting Department, Almaty, Kazakhstan

ARTICLE INFO

Article history:
Received 7 January 2007
Received in revised form
20 June 2008
Accepted 3 July 2008
Available online 20 August 2008

Keywords:
Brightness index
Grazing gradient
Kazakhstan
Kizalkum desert
Kriging
Land-use land-cover change
Landsat
Remote sensing
Semi-variogram
Ust-Urt Plateau

ABSTRACT

Soil and vegetation degradation around watering points has been observed in many drylands around the world. It can be recognized in spaceborne imagery as radial brightness belts fading as a function of distance from the water wells. The primary goal of the study was to characterize spatial and temporal land degradation/rehabilitation in the Central Asian drylands. Tasseled Cap's brightness index was found to be the best spectral transformation for enhancing the contrast between the bright-degraded areas close to the wells and the darker surrounding areas far from and in-between these wells. Semi-variograms were derived to understand the spatial structure present in the spaceborne imagery of two desert sites and in three key time periods (mid-late 1970s, around 1990, and 2000). A geostatistical model, namely the kriging interpolation technique, was applied for smoothing brightness index values extracted from 30 to 80 m spatial resolution images in order to assess spatial and temporal land-cover patterns. Change detection analysis, based on the kriging prediction maps, was performed to assess the direction and intensity of changes between the study periods. These findings were linked to the socio-economic situation before and after the collapse of the Soviet Union that influenced the grazing pressure and hence the land-use/land-cover state of the study sites.

The study found that degradation occurred in some areas due to recent exploration and exploitation of the gas and oil reserves in the region. Another area was subject to rehabilitation of the rangeland due to a dramatic decrease in the number of livestock due to socio-economical changes after the independence of Kazakhstan in 1991.

1. Background

According to the United Nations Environment Program (UNEP) the term *overgrazing* refers to a practice of allowing a much larger number of animals to graze at a location than it can actually support. As a result, overgrazing by different types of livestock is perhaps the most significant anthropogenic activity that degrades rangelands and causes desertification in terms of plant density, plant chemical content, community structure, and soil erosion (Manzano and Návar, 2000). Globally, about 75 million ha of land are strongly degraded by overgrazing, i.e. the original biotic functions are largely destroyed

* Corresponding author. Tel.: +972 8 6596855; fax: +972 8 6596805.
E-mail address: karnieli@bgu.ac.il (A. Karnieli).

0140-1963/$ - see front matter © 2008 Elsevier Ltd. All rights reserved.
doi:10.1016/j.jaridenv.2008.07.009

(Sinha, 1998). In arid and semi-arid environments, land (soil and vegetation) degradation is particularly related to areas surrounding point-sources of water, either natural or artificial, such as wells or boreholes (Lange, 1969).

Domestic animals (sheep, goats, cattle, camels, yaks, and horses) prefer to graze in the vicinity of a watering point. When food is depleted in this area they move away from the source of water but return regularly to drink. Consequently, large numbers of individuals frequently concentrate around watering points; a density that decreases gradually with increasing distance from water (Friedel, 1997; Pickup et al., 1993). Typical grazing distance away from the watering point is 4–6 km, which can increase to 10 or even 20 km under extreme conditions (Dobie, 1980; Hodder and Low, 1978). Lange (1969) named the radial grazing pattern *piosphere*, derived from the Greek root 'pios' meaning 'drink'. Pickup and Chewings (1994) defined the term '*grazing gradient*' as "spatial patterns in soil or vegetation characteristics resulting from grazing activities and which are symptomatic of land degradation" (p. 598). Such degraded features have been observed in most of the pastoral drylands around the world.

Many studies based on ground measurements and/or interpretation of remotely sensed data have been carried out to monitor the spatial variability of grazing impacts on rangelands. Many biotic, abiotic, and environmental effects are listed in the literature (e.g., Brooks et al., 2006; James et al., 1999; Ludwig et al., 2001, 2004; Perkins and Thomas, 1993). In these studies, vegetation cover, species richness and diversity, and distribution of biological soil crusts were analyzed as a function of distance from the watering point. Other studies deal with soil chemistry and physical properties, as well as erosion impact and trampling gradient. Most of the ground-based measurements are determined by sampling schemes along transects and were carried out in plots varying in size between 1 and 100 m^2. These efforts have shown that methods which measure only restricted areas are greatly affected by natural variation in vegetation composition and landscape characteristics that cannot reliably be related to the impact of grazing (Friedel et al., 1993). Conventional ground-based measurements are time consuming, relatively expensive, and the distant sites are not accessible for frequent repeatable sampling (Pickup and Chewings, 1994). Friedel (1997) assumed that the grazing effects cannot be monitored when the measurement is carried out only in a small spatial dimension. These difficulties are magnified when working in semi-arid rangelands, but remotely sensed data can overcome these problems.

For this reason, and since the radial pattern around watering points is well observed from space, most recent studies have been based on interpretation and modeling of remotely sensed data, which can be analyzed in a semi-automated and repeatable way over vast and remote areas. Various remote-sensing models, incorporating geographic information systems techniques, were developed to estimate the spatial distribution of different variables around watering points (Bastin et al., 1993; Hanan et al., 1991; Harris and Asner, 2003; Pickup et al., 1993).

The ground and spaceborne observations described in the literature demonstrate not only that the grazing gradients are characterized by concentric circles around the watering points, but also that the spatial pattern of the measured biotic, abiotic, and environmental variables are distributed in a common fashion. Each variable has a low (or high) value near the center and changes exponentially as the distance increases. The most utilized variable is vegetation cover, which can be assessed by spectral vegetation indices such as the normalized difference vegetation index (NDVI), the soil adjusted vegetation index (SAVI), and Perpendicular Distance (PD54) (Harris and Asner, 2003; Lind et al., 2003; Pickup et al., 1993; Washington-Allen et al., 2004), grass and annuals production (Hanan et al., 1991; Trodd and Dougill, 1998), bush encouragement, soil pH, organic content, phosphate, and nitrate (Perkins and Thomas, 1993), soil nutrient concentrations, particularly potassium and phosphorus (Fernandez-Gimenez and Allen-Diaz, 2001), and track density (Pringle and Landsberg, 2004). Moreover, most of these observations show that the rate of improvement (or decline) of each variable does not change after several kilometers (usually 6 km) from the watering point. It should be noted that despite this "normal" response, in some cases three other types of response, termed inversed, composite, and complex gradients were also observed (Pickup et al., 1994; Washington-Allen et al., 2004). Composite gradient is generally associated with invading species that replaced the palatable ones near the watering point. Inverse gradient is generally associated with a dam in area of predominantly woody vegetation, with higher vegetation signal, in the watering point. Complex gradient appears in area where reduced growth of vegetation in runoff and eroded areas is offset by increased growth in run-on and sediment sinks. Perkins and Thomas (1993) summarized the radial pattern of the grazing effects on vegetation and soil in the following belts—up to 50 m from the borehole is the *sacrifice zone* where most of the vegetation is destroyed and the surface is scattered by wind erosion; up to 800 m is the *nutritious grass zone*, dominated by palatable and grass species; up to 2000 m is the *bush encroachment zone*. According to these authors, this distance is the limit of major grazing effects.

Intensive grazing around watering points is a world-wide phenomenon, but the current study was conducted in the drylands of Kazakhstan with respect to the socio-economic transition that this country experienced at the end of the 20th century. Livestock farming is one of the main branches of the Kazakh economy. About 70% of the agricultural lands of Kazakhstan are used as year-around natural desert and semi-desert pastures. In the 1920s, under the influence of Soviet collectivization, the traditional family and tribal-oriented nomadic pastoral system was transformed, as all arable and rangeland were consolidated into large state-owned farms or collectives. Rangelands were overgrazed and mismanaged with specialized commercial production oriented towards exporting livestock products to Russia. In 1980, 60% of the Kazakh rangelands were under different degrees of degradation (Kharin and Kiriltseva, 1988; Robinson et al., 2003).

A drastic decline in livestock population happened after 1991 due to changes in the political system and collapse of the national economy (Alaolmolki, 2001). Unparallel land-use and land-cover changes occurred in the region. On one hand, due to shifts in profession (more agriculture) and the necessity to be close to the markets, more people were forced to migrate to the vicinity of central villages and towns. This process aggravated the ecological situation due to overgrazing and

vegetation cutting in these sites. On the other hand, less human activity exists in the remote areas. The previous strong centralized government subsidy programs were terminated, including the practice of guaranteed supplemental forage in cold winters and drought years. Farmers could no longer feed their livestock during the harsh winters, water wells were demolished, pumps were stolen or broken, and there were no longer means of transportation to convey the animals to the markets in the central cities (Antonchikov et al., 2002). Disengagement from Russia also led to decline in production of exports including wool and meat (Alaolmolki, 2001). Due to raising meat, wool, and milk prices (Kerven and Behnke, 1996), the diets of Kazakh people changed, as people ate more carbohydrates than meat. For all these reasons, the number of cattle declined by about 50% while the number of sheep sharply decreased from 34 million to less than 10 million head (Baydildina et al., 2000; de Beurs and Henebry, 2004; Robinson et al., 2003; Suleimenov and Oram, 2000). Consequently, drastic declines in livestock populations were observed after 1991 that have resulted in lower grazing pressure and hence recovery of the natural vegetation and rehabilitation of the land.

Another socio-economic process that characterizes the new independent state of Kazakhstan is accelerated development of the gas and oil industry. Kazakhstan, home to more than 2% of the world's proven oil reserves, is the second largest oil producer among the former Soviet republics after Russia, producing nearly 950,000 barrels per day, mostly from regions surrounding the Caspian Sea. Upon the breakup of the Soviet Union, the Kazakh government, recognizing the importance of foreign investment, implemented the most protracted effort to elicit such investments in its hydrocarbon resources as a cornerstone for development (Kadrzhanova, 2003; Ulmishek, 2001).

Remote-sensing studies of local desertification processes in Central Asia were carried out in the mid-1970s (Kharin and Kalenov, 1978; Vinogradov, 1976). Visual interpretation of the Soviet Souz photographs revealed more than 150 anthropogenic-induced desertification spots around the wells of south-east Karakum desert. The current paper presents another approach for assessing and mapping grazing impacts around watering points. The primary goal of the study was to characterize spatial and temporal land degradation/rehabilitation in the Central Asian drylands, in terms of vegetation and soil patterns, at different time periods, with respect to socio-economic changes. More specific objectives of the study were: (1) to derive semi-variograms in order to gain insight to the spatial structure present in the imagery of two desert sites and in three key different time periods (mid-late 1970s, late 1980s—early 1990s, and 2000); (2) to apply a geostatistical model, namely the kriging interpolation technique for smoothing brightness index values extracted from 30 to 80 m spatial resolution satellite images, in order to assess spatial and temporal land-cover patterns; (3) to conduct a change detection analysis based on kriging prediction maps to assess the direction and intensity of changes between the study periods; and (4) to link these findings to the socio-economic situation before and after the collapse of the Soviet Union that influenced the grazing intensity and hence the land-use/land-cover state of the study sites.

2. Procedures and methodology

2.1. Study sites

Two study areas are involved in the current research. Both are dryland steppe (rangeland) within the territory of Kazakhstan (Fig. 1). The climate is cold desert, typical to the mid-continental Asian deserts.

The Ust-Urt Plateau is located between the Aral Sea and the Caspian Sea (44°12′N, 54°24′E). It extends roughly 200,000 km^2, with an average elevation of 150 m, and is characterized by numerous stone debris plateaus with grey-brown

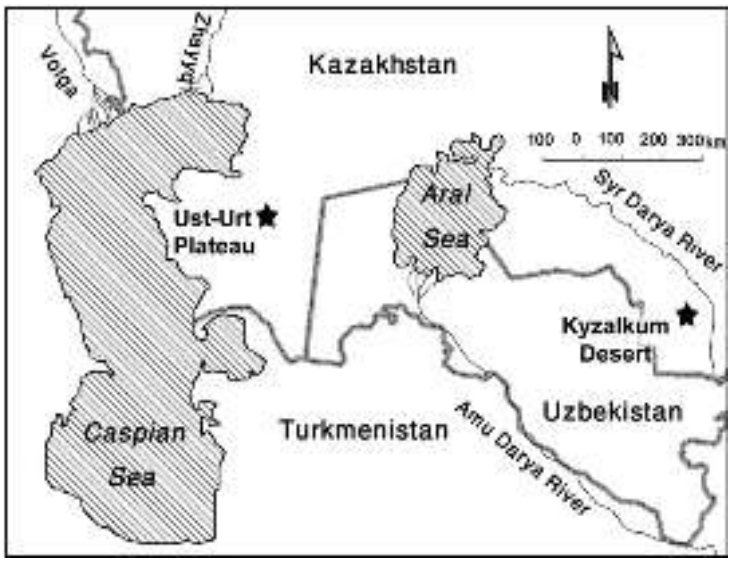

Fig. 1. Location map showing Ust-Urt Plateau and the Kyzylkum Desert in Kazakhstan. Stars indicate the study sites.

soils, solonchaks, and ridge and dune sands. The plateau's semi-nomadic population raises sheep, goats, camels, and horses. Vegetation is rather sparse, consisting of *Artemisia terrae albae*, *Salsola arbuscula*, and *Anabasis salsa*. The average annual temperature is about 12 °C; the absolute maximum and minimum are +42 and −40 °C, respectively. The average annual precipitation is 90 mm. The groundwater table is at a depth of 20–30 m.

The Kyzylkum Desert (43°25′N, 66°13′E) is the tenth largest desert in the world. Hillock and hillock-ridge sands characterize this area. The absolute heights within the research area range from 100 to 327 m above sea level. Water wells, located in the inter-ridge depressions, are the main source of water in the Kyzylkum Desert. The level of groundwater is 20–40 m, sometimes deeper. The water is slightly mineralized but suitable for livestock. Water resources rely only on local precipitation and ground water while no additional water is transferred to the region. The Kyzylkum Desert also belongs to the cold deserts belt of Asia. The mean annual precipitation is around 200 mm and temperatures range from below 0 °C in the winter to around 30 °C in the summer. Geobotanic mapping of the area that was conducted in 1973–1977 showed strong degradation of vegetation in the grazing areas. The dominant plant species near the settlements and watering points were *Ammodendron conollyi*, *Convulvus divaricatus*, *Cousinia*, *Artemisia scoparia*, *Artemisia razvesistaya*, *Astragalus paucijugus*, and *Heliotropum arguziodes.* The ephemeral cover included *Bromus tectorum*, *Ceratocephalus ortoceras*, *Diarthron vesiculosum*, and *Ceratocarpus arenarius*—indicators of degradation resulting from overgrazing.

Landsat images of the two study sites are presented in Fig. 2. These show the distribution of the watering points as bright spots spread over most of the area.

Three field surveys were carried out in the eastern part of the Kyzylkum Desert in 1973–1977, 1995, and 2001. Geobotanic mapping of the Kyzylkum Desert in the earliest period showed strong degradation of vegetation in the grazing areas. The repeated geobotanical mapping of Kyzylkum in 1995 revealed the rehabilitation processes of vegetation

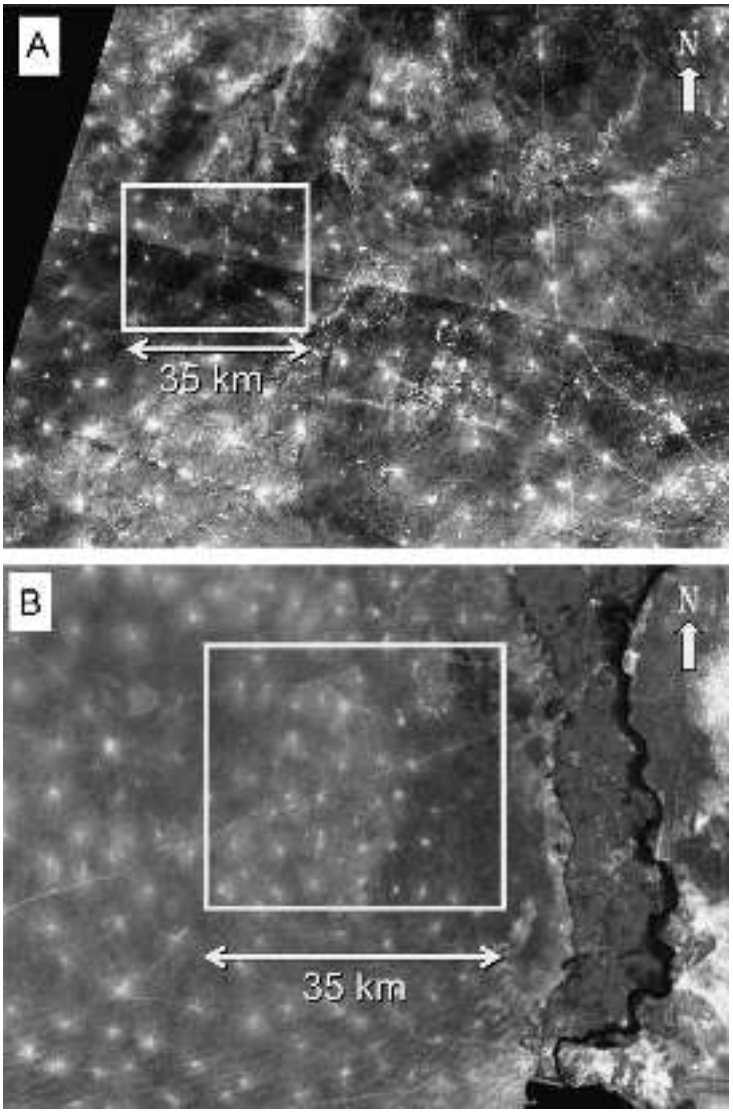

Fig. 2. Landsat TM false color images (R,G,B = 4,3,2) of the (A) Ust-Urt Plateau in 1987; (B) Kyzylkum Desert in 1991 where the agricultural fields along the Syr Darya River are shown on the right. In both images the bright spots are the sacrificed zones in the vicinity of watering points. The rectangles bound the specific sites where geostatistical analyses were preformed.

including recovery of herbaceous species. In June 2001, four watering points were chosen and a total of 19 sample plots in different directions and distances were analyzed. In addition, a cross-section between two wells that are still active was carried out. The Log Series Survey method established by McAuliffe (1990) was used for estimating the total vegetation cover for plant species in the research site.

2.2. Image processing

Six Landsat images (Table 1) covering the two study sites were downloaded from the Global Orthorectified Landsat Data by Landsat.Org (http://landsat.org/). The images were acquired by different sensors (MSS, TM, and ETM+) and are from three different time periods, as listed in Table 1. Subsets of the study fields were made, bounding an area of 1184 km^2 in the Ust-Urt Plateau and 1038 km^2 in the Kyzylkum Desert (Fig. 2). Livestock grazing is the only land-use practice in these sites.

Image processing started by converting image digital numbers to reflectance values (Chander and Markham, 2003; Markham and Barker, 1983; Williams, 2006). Reflectance values were used to calculate several vegetation indices for each image subset. These include the NDVI (Tucker, 1979), the SAVI (Huete, 1988), the modified SAVI (MSAVI, Qi et al., 1994), the perpendicular vegetation index (PVI, Richardson and Wiegand, 1977), and the tasseled cap-derived greenness and brightness indices (Kauth and Thomas, 1976). Spectral separability analysis, incorporating mean and standard deviation values of extreme classes in each scene, was applied to all indices in order to assess the most suitable index for differentiating between degraded and non-degraded land (Kaufman and Remer, 1994; Lasaponara, 2006). This analysis revealed that the brightness index (BI) produced the best separability value and consequently was selected for further analysis. The BI has the general form of

$$\mathrm{BI} = \alpha 1(B1) + \alpha 2(B2) + \ldots + \alpha n(Bn) \quad (1)$$

where Bn are the spectral band number and αn are the appropriate BI coefficients of each sensor—MSS, TM, and ETM+ (after Crist and Cicone, 1984; Huang et al., 2002; Kauth and Thomas, 1976, respectively). In addition to the above-mentioned statistically significant results, and the fact that this index was originally designed to examine soil properties, its advantage lies in its ability to compare different sensors with different spectral bands, as it subsets different spectral bands to one normalized layer of BI values.

In the next step, for the MSS, each window of 3×3 pixels was averaged to assign a new pixel value, and for the TM and ETM+, each window of 6×6 pixels was averaged for the same purpose. Thus, the resolution of the images was reduced by factors of 3 and 6, to fit the MSS and TM/ETM+ images, respectively. The resulting pixel size of 171 m was easily processed, as the subset size was reduced from approximately 1.5 million pixels to only 40,000 pixels. Note that even a pixel size of 171 m was assumed to be small enough for assessing changes within the 6 km from the watering point where degradation is expecting. Finally, although originally rectified, image-to-image geometric correction was applied for better accuracy in the forthcoming change detection procedure.

2.3. Geostatistical analysis

The key concept of geostatistics is that of the *regionalized variable* (Matheron, 1971), defined as a variable that can be characterized from a number of measurements that identify spatial structure. The basic assumption underlying this theory is that when assuming spatial continuity, samples that are located adjacent to one another tend to be more similar than samples located further apart. This spatially dependent variation may be treated statistically and described through a number of parameters derived from a *semi-variogram* that is the function relating the *semi-variance* to the directional distance between two samples. The semi-variance is defined as half the mean-squared difference between two samples a given direction and distance apart (Eq. (2)). The direction and distance are defined by the vector h that is commonly referred to as the *lag*:

$$\gamma(h) = \frac{1}{2N(h)} \sum_{i=1}^{N(h)} (z_{xi} - z_{xi+h})^2 \quad (2)$$

Table 1
Landsat images involved in the current research

Satellite/sensor	Location	Date	Path/row*
Landsat-2 MSS	Ust-Urt Plateau	April 25, 1975	176/29
Landsat-4 TM		June 14, 1987	163/29
Landsat-7 ETM+		June 9, 2000	163/29
Landsat-2 MSS	Kyzylkum Desert	September 4, 1979	167/31
Landsat-4 TM		August 4, 1991	155/31
Landsat-7 ETM+		August 4, 2000	155/31

* Path/row of the MSS images are listed according to Worldwide Reference System-1 (WRS-1) while those of TM and ETM+ are according to WRS-2.

where $\gamma(h)$ is the semi-variance at lag h, $N(h)$ is the number of sample-pairs a distance h apart, and Z_i is the value of the regionalized variable at location i. An idealized semi-variogram along with its associated features is illustrated in Fig. 3. In addition to the lag, the variogram is characterized by three other parameters—the nugget, range, and sill. The *nugget* is variability at zero distance and represents sampling and analytical errors. The *range* of influence designates the extent, say a distance a, beyond which autocorrelation between sampling sites is negligible. The *sill* represents the variability of spatially independent samples. An empirical semi-variogram can be calculated from the given set of observations and then a theoretical model can be fitted (Delhomme, 1978, 1979). Among other theoretical models, a popular one is the *exponential model* of the form:

$$\gamma(h) = C_0 + C_1\left[1 - \exp\left(\frac{-3|h|}{a}\right)\right] \tag{3}$$

where a is the range, h is the lag, C_0 is the nugget, and C_0+C_1 equals the sill. To better understand the spatial structure presented in the imagery for a given date and location variogram analysis was applied to the studied sites. The rationale for using semi-variograms was the similarity in spatial structure of most of the above-mentioned variables, gradually increasing (or decreasing) as a function of the increasing distance from the watering point until reaching the limit of no grazing effects, and the typical shape of the variogram. Curran (1988) and Woodcock et al. (1988a, b) introduced the semi-variogram to remote sensing and discovered that the parameters of the variogram can be directly related to a feature in an image. In the current case, presence or absence of a sill can be an evidence for radial grazing pattern around the watering points. Finally, the level of the sill can be related to the homogeneity (lower variance) of the area. The lag distance can be related to the walking distance of livestock since beyond a certain distance (the range) observations appear independent.

In each subset, the empirical semi-variogram was calculated based on 40,000 pixels, and then the model that best fits to it was estimated. Parameters for the model were found by minimizing the square differences between the empirical semi-variogram values and the theoretical model one. Once the latter was chosen, several criteria were applied to determine the correctness of the model and to adjust its parameters:

(1) Cross-validation scatter plot—in this plot, the measured and predicted data are regressed and the cloud of points is compared to a 1:1 line and to a line of best fit.
(2) Mean estimation error:

$$\frac{1}{n}\sum_{i=1}^{n}(Z_{xi} - Z^*_{xi}) = \frac{1}{n}\sum_{i=1}^{n}\varepsilon_i \approx 0 \tag{4}$$

where ε is the difference between the estimated and the known point value (this term should approach 0).
(3) Mean standardized squared estimation error:

$$\frac{1}{n}\sum_{i=1}^{n}\left[\frac{(Z_{xi} - Z^*_{xi})}{s^*_i}\right]^2 = \frac{1}{n}\sum_{i=1}^{n}\left(\frac{\varepsilon_i}{s_i}\right)^2 \approx 1 \tag{5}$$

where s^*_i is the estimation standard deviation (this term should approach 1).

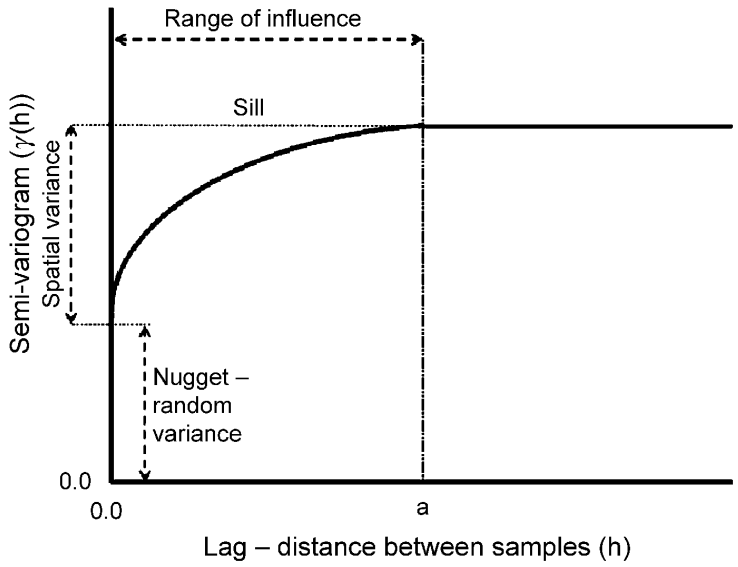

Fig. 3. An idealized semi-variogram along with the involved parameters.

A linear geostatistical technique, known as *ordinary kriging* interpolation, was used to reduce local effects and to provide a smoother surface than the surface brightness values in the study sites. This helps to better identify spatial phenomena. Ordinary kriging estimates the mean as a constant in the searching neighborhood (Isaacs and Srivastava, 1989). The kriging technique has recently become very common for analyzing spaceborne data (Oliver et al., 2000).

2.4. Image differencing change detection analysis

A post-processing change detection method, hereafter the BI differencing method, a variant of the vegetation index differencing method (Jensen, 1986; Yuan et al., 1998) was implemented to assess the main trends of degradation/rehabilitation in the study sites. For each site, the two pairs of kriging maps (i.e., 1987–1975 and 2000–1987 for Ust-Urt Plateau, and 1991–1979 and 2000–1991 for Kyzylkum Desert) were differenced ($\Delta BI = BI_{t+1} - BI_t$ where t and t+1 are the two time periods).

The relative change in trends during the three decades under study was investigated by categorizing the direction and the level of change using a threshold of 1 standard deviation, according to

$$\text{Change} = \begin{cases} -2 \text{ if } \Delta BI < -2STD \cdots \text{high rehabilitation (HR)} \\ -1 \text{ if } \Delta BI \leqslant -1STD \cdots \text{low rehabilitation (LR)} \\ 0 \text{ if } -1STD \leqslant \Delta BI < 1STD \cdots \text{no change} \\ 1 \text{ if } \Delta BI \geqslant 1STD \cdots \text{low degradation (LD)} \\ 2 \text{ if } \Delta BI \geqslant 2STD \cdots \text{high degradation (HD)} \end{cases} \quad (6)$$

where STD is standard deviation from the mean difference. Note that the only way to detect absolute changes is by extensive field observations. Unfortunately, such data for this long period of time was not available. Therefore, changes presented in this study are relative changes from which the general trends can clearly be extracted.

3. Results and discussion

3.1. Geostatistical analysis

To avoid redundancy, details of the analysis procedure are exemplified only for the Ust-Urt Plateau site, followed by results for the both sites. Fig. 4 shows the respective BI products, calculated by Eq. (1), with the appropriate coefficients. Watering points are recognized as bright spots spread over most of the 1970s and 1980s images, but hardly appear in the 2000 ones. In the latter image of the Ust-Urt Plateau many of the watering points have disappeared; however, a wide bright area exists in the center of the image (Fig. 4c). Similarly, in the same year, at the Kyzylkum Desert site, most of the previously observed watering points cannot be seen any more (Fig. 4f). High BI values correspond to bare, degraded, soil. The brightness levels were equally stretched for the different sensors. BI values range from 0.65 to 0.96 and from 0.19 to 0.56 for the Ust-Urt and the Kyzylkum sites, respectively.

All six BI images were used for the geostatistical analysis. First, empirical semi-variograms for the three periods, for each of the two sites, were established (six sub-images altogether). In field observations, no evidence was found to support anisotropic pattern, such as linear dunes or other barriers that may govern the grazing direction of the livestock. Consequently, isotropic distribution was assumed in all cases. Results of the cross-validation analyses are presented in Table 2. The slope coefficient is very close to unity and the intercept coefficient is very close to zero, proving the ability of the chosen exponential model to reproduce the observed values.

Subsequently, several theoretical models (Delhomme, 1978) were examined and the *exponential model* (Eq. (3)) was selected due to the best cross-validation results. The least-squares measure of fit was used, incorporating exponential models, as shown in Fig. 5. The variogram parameters are presented in Table 2. All variograms were processed with 16 lags of 1000 m each. Lag values were determined by trail and error process to optimize the above-mentioned criteria. Visually, the 1975 and 1987 variograms look quite similar, having a typical variogram shape. Two features can be noticed. Firstly, the sill of the 1987 variogram is lower than 1975 one, indicating lower variance in the former year. Also, in 1975 the range is 6000 m and in 1987 it is 7000 m, which matches the reported walking distance of livestock from their drinking source (Dobie, 1980; Hodder and Low, 1978). On the contrary, the 2000 variogram reaches about the same sill level only after 16,000 km. Such a range does not seem to be indicative to the grazing pattern in the region.

Next, kriging interpolation maps were produced based on the exponential models with the parameters presented in Table 2. Fig. 6 depicts the final products for the distribution of the BI values for the three periods, for both sites. In the early maps ($\leqslant$1991) one can observe the belts around the watering points, indicating progressive land degradation radiating from the wells, i.e., the grazing gradient. The dark-red areas in the images are related to zones where the grazing impact is the predominant feature that has a strong effect on the spatial variation. These areas can be considered as the center of the grazing impact, denoted as the '*sacrifice zone*' by Perkins and Thomas (1993). The surrounding light red and yellow belts represent a mixed zone where grazing impact and natural variability overlay each other or create a stable balance. This zone can be compared to an edge zone of the grazing impact and highlights the principal migration routes of livestock. The zone colored by blue tones is considered to be an area where natural variability overbalances the grazing impact, denoted

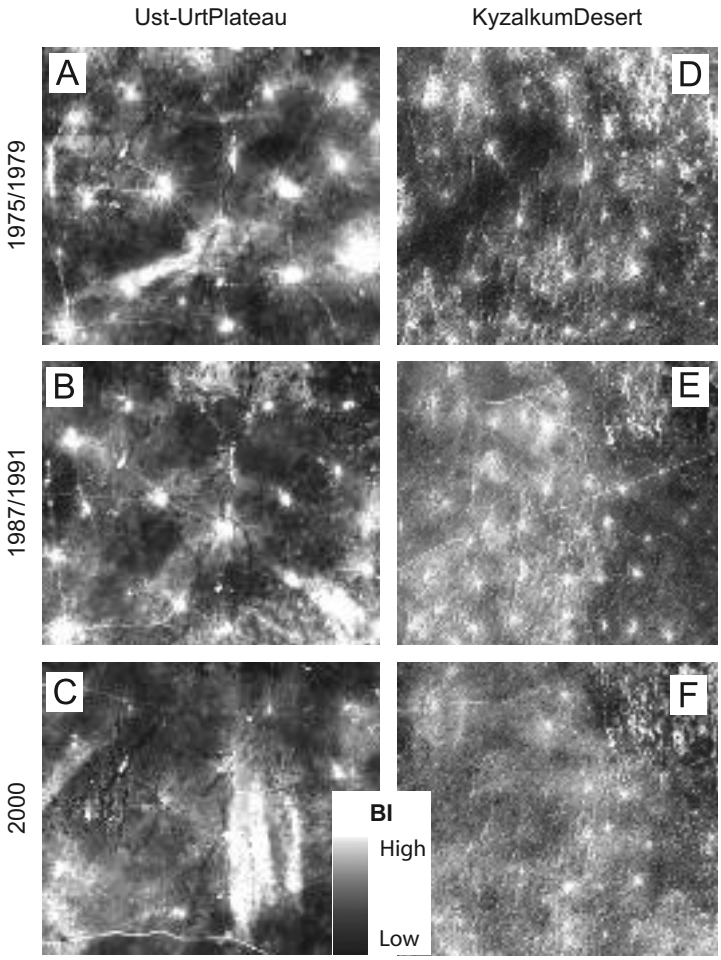

Fig. 4. Brightness index products: (A) Ust-Urt Plateau in 1975, (B) Ust-Urt Plateau in 1987, (C) Ust-Urt Plateau in 2000, (D) Kyzylkum Desert in 1979, (E) Kyzylkum Desert in 1991, and (F) Kyzylkum Desert in 2000. Dimension of each panel is about 35 × 30 km.

Table 2
Variogram parameters for the exponential models fitting the BI subset products for the Ust-Urt Plateau for the three periods and their cross-validation values

	Ust-Urt Plateau		
	1975	1987	2000
Nugget	0.00	0.00	0.00
Sill	0.0011	0.0008	0.0010
Lag (m)	1000	1000	1000
Range (m)	5952.9	7137.4	15953.0
Root-mean-square	0.0095	0.0096	0.0096
Average standard error	0.0096	0.0121	0.0111
Mean standardized	0.00008	−0.00063	−0.00006
Root-mean-square standardized	0.9883	0.7935	0.8701

as '*grazing reserve*' by Perkins and Thomas (1993). The radial pattern, related to the grazing gradient, is not seen in the 2000 map. Instead, the dominant feature in the middle of the scene is colored in by red tones.

3.2. Image differencing change detection analysis

The BI differencing method (detailed in Section 2.4) was implemented to understand temporal trends in the grazing patterns during these two periods. The change detection maps and their respective frequency histograms are presented in Fig. 7. In the 1987–1975 change detection map and histogram of Ust-Urt Plateau (Fig. 7a and b) much of the area is black, indicating no change in the grazing patterns. Of the rest, only a few small and local spots are orange-brown, representing degradation, and the remaining area has green tones, representing rehabilitation. The general trend from the late 1970s to

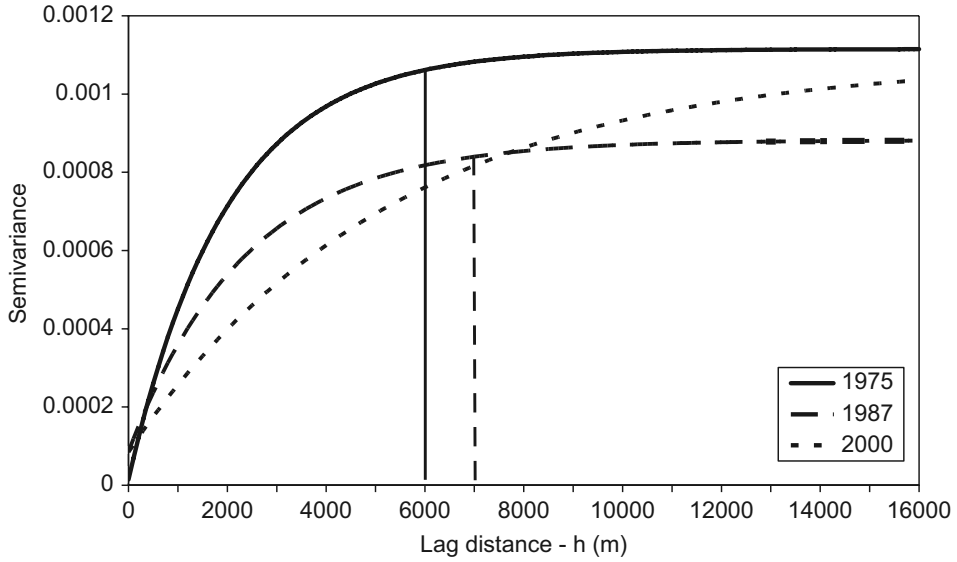

Fig. 5. Model variograms for the brightness index values of the Ust-Urt Plateau in 1975, 1987, and 2000.

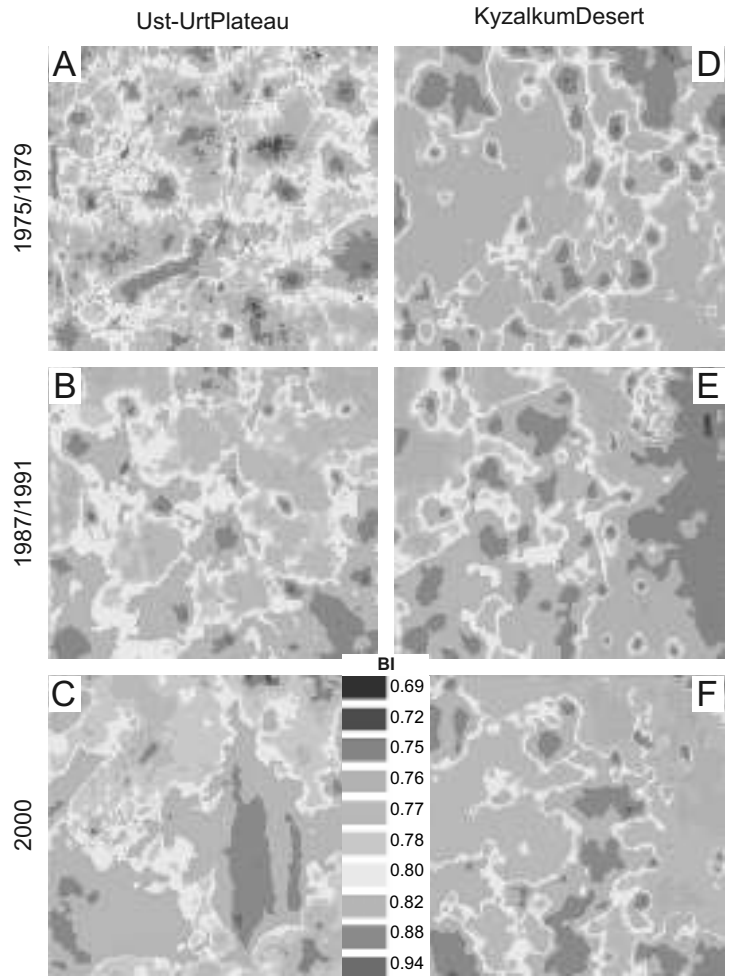

Fig. 6. Kriging interpolation maps for images shown in Fig. 3 based on the brightness index values: (A) Ust-Urt Plateau in 1975, (B) Ust-Urt Plateau in 1987, (C) Ust-Urt Plateau in 2000, (D) Kyzylkum Desert in 1979, (E) Kyzylkum Desert in 1991, and (F) Kyzylkum Desert in 2000. Dimension of each panel is about 35×30 km.

the late 1980s, therefore, was towards favorable land-cover conditions, or rehabilitation. Note also that in 1987 the area was more homogenous as is reflected by the lower sill in Fig. 5 and by the smaller color range in Fig. 6b. An opposite trend was detected in the second period (2000–1987), when degradation processes (warm colors) characterized a considerable

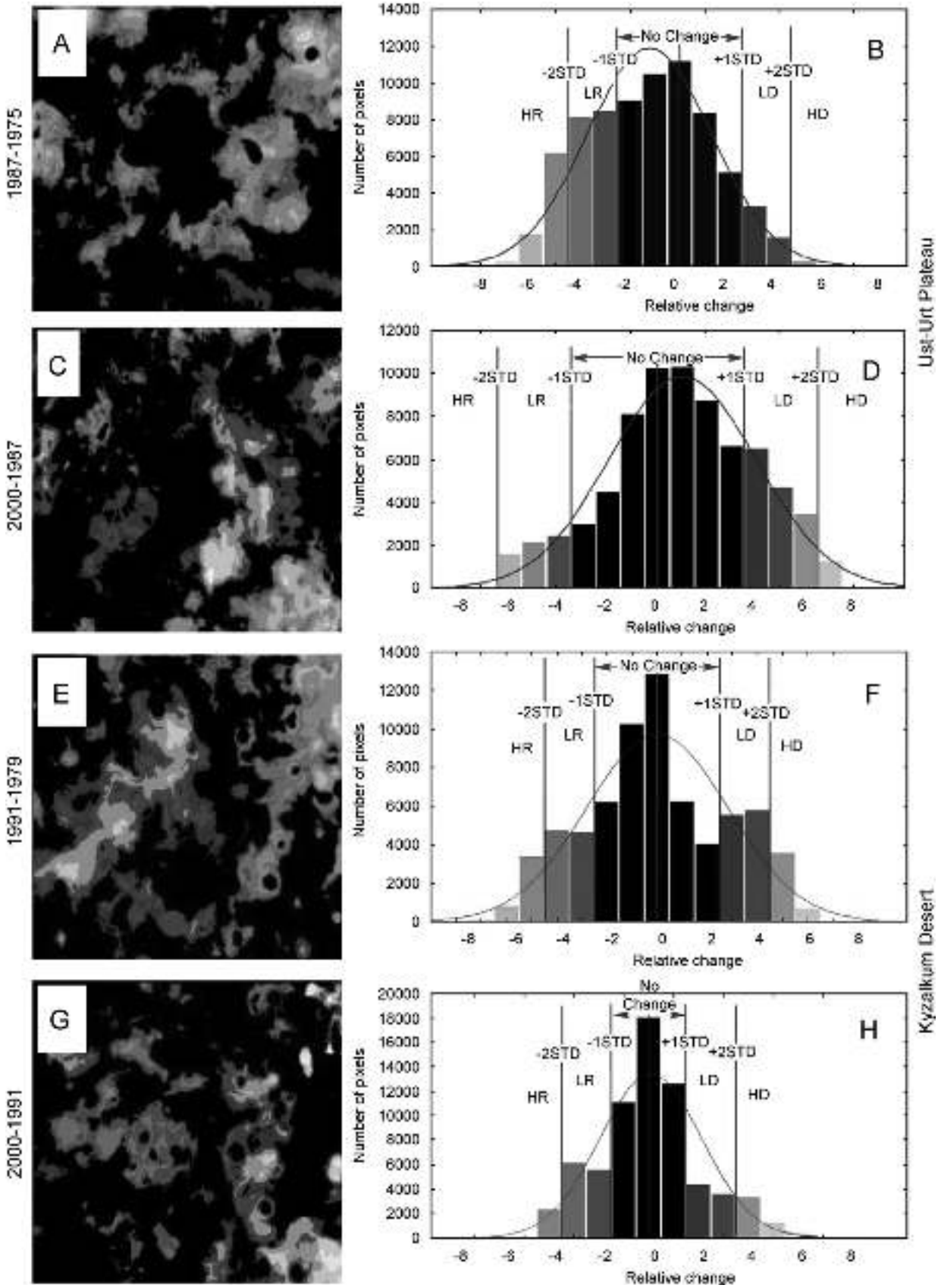

Fig. 7. Change detection results shown as maps and histograms: HR = high rehabilitation, LR = low rehabilitation, HD = high degradation, LD = low degradation. (A and B) Difference between the 1987 and 1975 images for the Ust-Urt Plateau; (C and D) difference between the 2000 and 1987 images for the Ust-Urt Plateau; (E and F) difference between the 1991 and 1979 images for the Kyzylkum Desert; (G and H) difference between the 1991 and 1979 images for the Kyzylkum Desert. Dimension of panels A, C, E, and G is about 35 × 30 km.

proportion of the area, while rehabilitation (green tones) covered a significantly smaller area (Fig. 7c and d). This is thought to be as a result of exploration and exploitation of gas and oil reserves in this region after the collapse of the Soviet Union and the establishment of Kazakhstan as an independent state in 1991 (Kadrzhanova, 2003; Ulmishek, 2001). Consequently, large areas underwent intensive land conversion, i.e. increased use of large amounts of heavy-duty equipment, large-scale plants, and vehicles that damage the soil surface (R. Mirzadinov, pers. comm.).

The Kyzylkum Desert represents another example of how different socio-economic situations before and after the independence of the former Soviet states can cause significant land-use and land-cover changes. Here the difference map and histogram computed from 1991 to 1979 show mixed changes (Fig. 7e and f). In the second period (2000–1991), the western side of the study area was rehabilitated (Fig. 7g and h). This is due to the difficult economic conditions that prevailed with the transition reforms that led to several major socio-economic changes. As explained in Section 1, after 1991 the number of livestock declined dramatically and thus the grazing pressure, leading to recovery of the natural vegetation and rehabilitation of the land. A similar trend was described by de Beurs and Henebry (2004) in other grassland and pasture areas in Kazakhstan. Although, most of the grazing in the Kyzylkum Desert has deceased, some minor activity remained, concentrated in the eastern side of the research site close to the agricultural area along the Syr-Darya River (Fig. 2b). The field survey in 2001 evidenced several active wells and heavy grazing pressure in this area that can be observed as the degraded part in Fig. 7g and h.

4. Conclusions

The current paper sought to characterize the spatial and temporal land degradation/rehabilitation in the Central Asian drylands, in terms of vegetation and soil patterns, at different time periods, with respect to socio-economic changes that happened after the collapse of the Soviet Union. The tasseled cap-derived brightness index (BI) was selected to describe the spatial surface patterns since (1) it produced the best contrast in terms of separability among all examined spectral indices; (2) it was originally designed to examine soil properties; and (3) it is able to compare between the different sensors with different spectral bands, as it reduces their different spectral bands to one normalized layer of BI values.

Geostatistical analysis in terms of semi-variance analysis was found to be a suitable method for gaining insight to the spatial structure present in the imagery for a given date and location. The similarity between the shape of the variogram and the directional change of many biotic, abiotic, and environmental variables along the grazing gradient radiated from the watering points in arid and semi-arid regions is a logical reason for using this method. The variogram models of the 1970 and the 1980s enable quantitative generalization of the phenomena over the region under interest. An average range of 6000–7000 m matches the reported walking distance of livestock from their drinking source. Comparison between variograms from different years can hint about the temporal dynamic of the region since when grazing stopped in the 1990s, the variogram did not reach a sill.

The kriging interpolation technique was used as a smoothing filter in which each pixel is being replaced with the solution for the variogram equation (exponential model in the current case) calculated from all other pixels in the image. As a result, it reduces spatial errors and fine scale variability and helps to better identify the degradation boundaries around the watering points. A radial pattern, indicating progressive land degradation radiating from the wells, namely the grazing gradient, is observed in the maps preceding the disengagement of Kazakhstan from Russia. This pattern is blurred or does not exist in the 2000 maps. In comparison with other interpolation techniques the ordinary kriging is considered to be the best linear unbiased estimator.

Temporal changes were effectively conducted by the index differencing technique. The study demonstrates the ability of spaceborne image analysis to follow after land-use/land-cover changes caused by dramatic socio-economic changes as occurred in Kazakhstan after its separation from Russia. Different effects are observed. One part of the state was degraded due to recent exploration and exploitation of the gas and oil reserves, while another part underwent rehabilitation processes due to dramatic reduction of the grazing pressure.

Acknowledgment

This research was supported by the EC Grant "Effect of biogenic crusts on biomass estimation in arid regions by satellite imagery" (INTAS-96-1833).

References

Alaolmolki, N., 2001. Life After the Soviet Union, The Newly Independent Republics of the Transcaucasus and Central Asia. State University of New York Press, Albany, NY.

Antonchikov, A.N., Bakinova, T.I., Dushkov, V.Y., Zalibekov, Z.G., Levykin, S.V., Neronov, V.M., Okolelova, A.A., Pazhenkov, A.S., Cherniakhovsky, D.A., Chibilev, A.A., 2002. Desertification and Ecological Problems of Pasture Stockbreeding in the Steppe Regions of Southern Russia. IUCN—World Conservation Union, Moscow, 88pp.

Bastin, G.N., Pickup, G., Chewings, V.H., 1993. Land degradation assessment in central Australia using a grazing gradient method. Rangeland Journal 15, 190–216.

Baydildina, A., Akshinbay, A., Bayetova, M., Mkrytichyan, L., Haliepesova, A., Ataev, D., 2000. Agricultural policy reforms and food security in Kazakhstan and Turkmenistan. Food Policy 25, 733–747.
Brooks, M.L., Matchett, J.R., Berry, K.H., 2006. Effects of livestock watering sites on alien and native plants in the Mojave Desert, USA. Journal of Arid Environments 67, 125–147.
Chander, G., Markham, B., 2003. Revised Landsat-5 TM radiometric calibration procedures and postcalibration dynamic ranges. IEEE Transactions on Geoscience and Remote Sensing 41, 2674–2677.
Crist, E.P., Cicone, R.C., 1984. A physically-based transformation of Thematic Mapper data—the TM tasseled cap. IEEE Transactions on Geoscience and Remote Sensing 22, 256–263.
Curran, P.J., 1988. The semivariogram in remote sensing: an introduction. Remote Sensing of Environment 24, 493–507.
de Beurs, K.M., Henebry, G.M., 2004. Land surface phenology, climatic variation, and institutional change: analyzing agricultural land cover change in Kazakhstan. Remote Sensing of Environment 89, 497–509.
Delhomme, J.P., 1978. Kriging in the hydroscience. Advances in Water Resources 1, 251–266.
Delhomme, J.P., 1979. Spatial variability and uncertainty in groundwater flow parameters: a geostatistical approach. Water Resources Research 15, 269–280.
Dobie, J.F., 1980. The Longhorns. University of Texas Press, 186pp.
Fernandez-Gimenez, M., Allen-Diaz, B., 2001. Vegetation change along gradients from water sources in three grazed Mongolian ecosystems. Plant Ecology 157, 101–118.
Friedel, M.H., 1997. Discontinuous change in arid woodland and grassland vegetation along gradients of cattle grazing in Central Australia. Journal of Arid Environments 37, 145–164.
Friedel, M.H., Pickup, G., Nelson, D.J., 1993. The interpretation of vegetation change in a spatially and temporally diverse arid Australian landscape. Journal of Arid Environments 24, 241–260.
Hanan, N.P., Prevost, Y., Diouf, A., Diallo, O., 1991. Assessment of desertification around deep wells in the Sahel using satellite imagery. Journal of Applied Ecology 28, 173–186.
Harris, A.T., Asner, G.P., 2003. Grazing gradient detection with airborne imaging spectroscopy on a semi-arid rangeland. Journal of Arid Environments 55, 391–404.
Hodder, R.M., Low, W.A., 1978. Grazing distribution of free-ranging cattle at three sites in the Alice Spring district, Central Australia. Australian Rangeland Journal 1, 95–105.
Huang, C., Wylie, B., Yang, L., Homer, C., Zylstra, G., 2002. Derivation of a tasseled cap transformation based on Landsat 7 at-satellite reflectance. International Journal of Remote Sensing 23, 1741–1748.
Huete, A.R., 1988. A soil-adjusted vegetation index (SAVI). Remote Sensing of Environments 25, 295–309.
Isaacs, E., Srivastava, M.R., 1989. An Introduction to Applied Geostatistics. Oxford University Press, New York, 592pp.
James, C.D., Landsberg, J., Morton, S.R., 1999. Provision of watering points in the Australian arid zone: a review of effects on biota. Journal of Arid Environments 41, 87–121.
Jensen, J.R., 1986. Introductory Digital Image Processing, A Remote Sensing Perspective. Prentice-Hall, New Jersey, 379pp.
Kadrzhanova, A., 2003. International Market Research—Oil and Gas Field Equipment. Industry Canada. Available at: 〈http://strategis.ic.gc.ca/epic/internet/inimr-ri.nsf/en/gr114924e.html〉. Accessed 3 December 2006.
Kaufman, Y.J., Remer, L.A., 1994. Detection of forests using MID-IR reflectance—an application for aerosol studies. IEEE Transactions on Geoscience and Remote Sensing 32, 672–683.
Kauth, J., Thomas, G.S., 1976. The tasseled cap—a graphic description of the spectral-temporal development of agricultural crops as seen by LANDSAT. In: Proceedings of the Symposium on Machine Processing of Remotely Sensed Data. Purdue University of West Lafayette, Indiana, pp. 4B-41–4B-51.
Kerven, C., Behnke, R., 1996. Impacts of decollectivization on rangelands and livestock marketing in Central Asia. In Small Ruminant/Global Livestock CRSP, Central Asia, Regional Livestock Assessment. Management Entity, Small Ruminant CRSP. University of California, Davis, CA, pp. 89–106.
Kharin, N.G., Kalenov, G.S., 1978. Study of anthropogenic desertification by satellite imagery. Problems of Desert Development 4, 25–29.
Kharin, N.G., Kiriltseva, A.A., 1988. New data on areas of desertified lands in the arid zone of the USSR. Problems of Desert Development 4, 3–8.
Lange, R.T., 1969. The piosphere: sheep track and dung patterns. Journal of Range Management 22, 396–400.
Lasaponara, R., 2006. Estimating spectral separability of satellite derived parameters for burned areas mapping in the Calabria region by using SPOT-Vegetation data. Ecological Modelling 196, 265–270.
Lind, M., Rasmussen, K., Adriansen, H., Ka, A., 2003. Estimating vegetative productivity gradients around watering points in the rangelands of Northern Senegal based on NOAAAVHRR data Geografisk Tidsskrift, Danish. Journal of Geography 103, 1–15.
Ludwig, J.A., Coughenour, M.B., Liedloff, A.C., Dyer, R., 2001. Modelling the resilience of Australian savanna systems to grazing impacts. Environment International 27, 167–172.
Ludwig, J.A., Tongway, D.J., Bastin, G.N., James, C.D., 2004. Monitoring ecological indicators of rangeland functional integrity and their relation to biodiversity at local to regional scales. Austral Ecology 29, 108–120.
Manzano, M.G., Návar, J., 2000. Process of desertification by goats overgrazing in the *Tamaulipan thornscub* (matorral) in north-eastern Mexico. Journal of Arid Environments 44, 1–17.
Markham, B.L., Barker, J.L., 1983. Spectral characterization of the Landsat-4 MSS sensors. Photogrammetric Engineering and Remote Sensing 49, 811–833.
Matheron, G., 1971. The Theory of Regionalized Variables and Its Applications, Cahiers du Centre de Morphologie Mathematique de Fontainebleau, No. 5, Ecole Superieure des Mines, Fontainebleau, 211pp.
McAuliffe, J.R., 1990. A rapid survey method for the estimation of density and cover in desert plant communities. Journal of Vegetation Science 1, 653–656.
Oliver, M.A., Webster, R., Slocum, K., 2000. Filtering SPOT imagery by kriging analysis. International Journal of Remote Sensing 21, 735–752.
Perkins, J.S., Thomas, D.S.G., 1993. Spreading deserts or spatially confined environmental impacts: land degradation and cattle ranching in the Kalahari desert of Botswana. Land Degradation and Rehabilitation 4, 179–194.
Pickup, G., Chewings, V.H., Nelson, D.J., 1993. Estimating changes in vegetation cover over time in arid rangelands using Landsat MSS Data. Remote Sensing of Environments 43, 243–263.
Pickup, G., Bastin, G.N., Chewings, V.H., 1994. Remote-sensing-based condition assessment for nonequilibrium rangelands under large-scale commercial grazing. Ecological Applications 4, 497–517.
Pickup, G., Chewings, V.H., 1994. A grazing gradient approach to land degradation assessment in arid areas from remotely sensed data. International Journal of Remote Sensing 15, 597–617.
Pringle, H.J.R., Landsberg, J., 2004. Predicting the distribution of livestock grazing pressure in rangelands. Austral Ecology 29, 31–39.
Qi, J., Chehbouni, A., Huete, A.R., Kerr, Y.H., Sorooshian, S., 1994. A modified soil adjusted vegetation index. Remote Sensing of Environments 48, 119–126.
Richardson, A.J., Wiegand, C.L., 1977. Distinguishing vegetation from soil background information. Photogrammetric Engineering and Remote Sensing 43, 1541–1552.
Robinson, S., Milner-Gulland, E.J., Alimaev, I., 2003. Rangeland degradation in Kazakhstan during the Soviet era: re-examining the evidence. Journal of Arid Environments 53, 419–439.
Sinha, P.C. (Ed.), 1998. Desertification. International Encyclopedia of Sustainable Development Series. Anmol Publications Pvt. Ltd., New Delhi.
Suleimenov, M., Oram, P., 2000. Trends in feed, livestock production, and rangelands during the transition period in three Central Asian countries. Food Policy 25, 681–700.
Trodd, N.M., Dougill, A.J., 1998. Monitoring vegetation dynamics in semi-arid African rangelands—use and limitations of Earth observation data to characterize vegetation structure. Applied Geography 18, 315–330.

Tucker, J.C., 1979. Red and photographic infrared linear combination for monitoring vegetation. Remote Sensing of Environment 8, 127–150.
Ulmishek, G.F., 2001. Petroleum Geology and Resources of the North Caspian Basin, Kazakhstan and Russia. US Geological Survey Bulletin 2201-B, Denver, 26pp.
Vinogradov, B.V., 1976. Study of desertification forms by aerial and space imagery. Problems of Deserts Development 3–4, 35–44.
Washington-Allen, R.A., Van Niel, T.G., Ramsey, R.D., West, N.E., 2004. Remote sensing-based piosphere analysis. GIScience and Remote Sensing 41, 136–154.
Williams, D., 2006. Landsat-7 Science Data Users Handbook. Available at: 〈http://ltpwww.gsfc.nasa.gov/IAS/handbook/handbook_htmls/chapter11/chapter11.html〉. Accessed 3 December 2006.
Woodcock, C.E., Strahler, A.H., Jupp, D.L.B., 1988a. The use of the variogram in remote sensing: I. Scene models and simulated images. Remote Sensing of Environments 25, 323–348.
Woodcock, C.E., Strahler, A.H., Jupp, D.L.B., 1988b. The use of the variogram in remote sensing: II. Real digital images. Remote Sensing of Environments 25, 349–379.
Yuan, D., Elvidge, C.D., Lunetta, R.S., 1998. Survey of multispectral methods for land cover change analysis. In: Lunetta, R.S., Elvidge, C.D. (Eds.), Remote Sensing. Change Detection: Environmental Monitoring. Methods and Application. Taylor and Francis Ltd., London, pp. 21–39, 318pp.